A semi-analytical study for moonpool resonance mitigation using a porous disk with a new pressure drop condition

Xingya Feng[1,*], **Javeria Ali**[1], **Xiaobao Chen**[2]
[1]Southern University of Science and Technology, Shenzhen, China
[2]Research Department, Bureau Veritas Marine & Offshore, France
*E-mail address of the presenting author: xingya.feng@sustech.edu.cn

1 Introduction

Porous or perforated plates are demonstrated to be effective in dissipating wave loads for offshore structures. A key issue for such application is the damping, mathematically, the pressure drop condition, induced by the porous plate/structure. Following the previous work in Chen et al [1] in the workshop in 2024, we employed their newly proposed pressure drop condition for the study of moonpool resonance problem. The internal resonance phenomena in moonpool structures have been studied by a number of researchers using semi-analytical methods based on eigenfunction expansions.

Miles and Gilbert [2] established the first theoretical contributions by studying wave scattering by a circular dock, while Garrett [3] was the very first to investigate a bottomless cylindrical moonpool structure. Mavrakos [4] performed a comprehensive study of the wave-induced forces that were exerted on a cylindrical structure with a finite wall thickness. The classical potential-flow theory remains unable to capture the significant resonant effects, although significant progress has been made within this framework. In order to reduce wave resonance in moonpools, pressure drop conditions have been used in prior studies; however, such studies required empirical calibration of the coefficients for the boundary conditions. To overcome the limitations of empirical pressure drop models, this work uses a newly proposed boundary condition that is based on the geometry of the disk, which eliminates the requirement for calibrating the coefficients. To address the diffraction boundary-value problem, the Galerkin method is employed to compute internal fluid motion within the cylindrical domain. The results show that the quadratic boundary condition is effective for mitigating the resonant behavior in the moonpool. This study provides a generalized structure and theoretical basis for viscous-inertial coupling in moonpool hydrodynamics.

2 Methodology

The velocity potential $\Phi(r, \theta, z, t)$ satisfies the Laplace equation in the fluid domain, since the flow is incompressible and irrotational:

$$\nabla^2 \Phi(r, \theta, z, t) = 0. \tag{1}$$

At $z = 0$, the linearized free-surface condition is given by $-f\Phi + \frac{\partial \Phi}{\partial z} = 0$, where $f = \dfrac{\omega^2}{g}$. No-flux conditions are imposed across the impermeable bottom and solid cylinder walls as $\frac{\partial \Phi}{\partial z}\big|_{z=-h} = 0$ and $\frac{\partial \Phi}{\partial n}\big|_{\text{walls}} = 0$. The Sommerfeld radiation condition provides a unique physical solution by guaranteeing that wave perturbations vanish at infinity.

At the entrance of the moonpool, we place a dissipative disk to introduce the dissipation effect. The pressure drop condition [1] is given by

$$\Delta p = \frac{14}{15}(1-\tau)C_g \rho u + \frac{1-\tau}{2\gamma\tau^2}\rho u|u| \tag{2}$$

where γ is the discharge coefficient [0.5,1.0], C_g is the group velocity, τ is the porosity parameter, and u is the velocity component normal to the porous disk surface. Note that this pressure drop condition includes a linear component and a quadratic one. The linear component accounts for the friction effect on the porous plate and the quadratic one explains the drag effect. The entire fluid region is divided into four subdomains (Fig. 1).

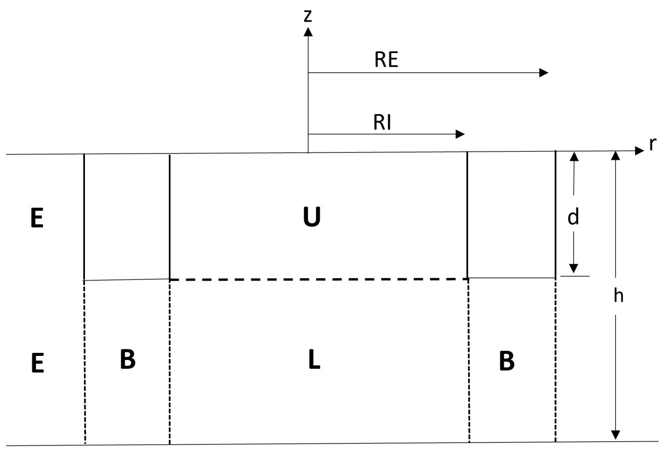

Figure 1: Schematic diagram of the moonpool system with a dissipative disk.

2.1 General Solution

Following Garrett [3], the velocity potential in the exterior subdomain E is written as

$$\phi_E^l(r,z) = a_0^l Z_0(k_0,z,h)\frac{H_l(k_0 r)}{H_l'(k_0 R_E)} + \sum_{n=1}^{\infty} a_n^l Z_n(k_n,z,h)\frac{K_l(k_n r)}{K_l'(k_n R_E)} + \Phi_0^l, \tag{3}$$

with

$$Z_0(k_0,z,h) = \frac{\cosh(k_0 h)\cos[k_0(z+h)]}{2k_0 h + \sinh(2k_0 h)}, \quad Z_n(k_n,z,h) = \frac{\cos(k_n h)\cos[k_n(z+h)]}{2k_n h + \sin(2k_n h)}. \tag{4}$$

The velocity potential in the below subdomain B can be expressed as

$$\begin{aligned}\phi_B^\ell(r,z) &= b_0^\ell G_0^\ell(r) + \sum_{n=1}^{\infty} b_n^\ell \left[K_I^{n\ell} I_\ell(\lambda_n r) - I_I^{n\ell} K_\ell(\lambda_n r)\right]\cos\lambda_n(z+h) \\ &+ \tilde{b}_0^\ell \tilde{G}_0^\ell(r) + \sum_{n=1}^{\infty} \tilde{b}_n^\ell \left[I_E^{n\ell} K_\ell(\lambda_n r) - K_E^{n\ell} I_\ell(\lambda_n r)\right]\cos\lambda_n(z+h),\end{aligned} \tag{5}$$

Next, the velocity potential ϕ_L^l in the lower interior subdomain L below the dissipative disk is expressed as:

$$\phi_L^l = \phi_I^l + \tilde{\phi}_L^l, \tag{6}$$

where the first term represents a transparent circular disk and is written as:

$$\phi_I^l = d_0^l Z_0(k_0, z, h)\frac{J_l(k_0 r)}{J_l'(k_0 R_I)} + \sum_{n=1}^{\infty} d_n^l Z_n(k_n, z, h)\frac{I_l(k_n r)}{I_l'(k_n R_I)}. \tag{7}$$

The second term, the Fourier-Bessel series, is given by:

$$\tilde{\phi}_L^l = \sum_{n=1}^{\infty} e_n^l \frac{\cosh[\chi_n^l(z+h)]}{\sinh[\chi_n^l(h-d)]}\frac{J_l(\chi_n^l r)}{J_l'(\chi_n^l R_I)}. \tag{8}$$

The wavenumber χ_n^l is the root of the positive zero of the Bessel function:

$$J_l(\chi_n^l R_I) = 0, \quad 0 < \chi_0^l < \cdots < \chi_n^l < \ldots \tag{9}$$

The velocity potential Φ_U^l in the upper interior domain U above the dissipative disk is expressed as the sum of two expansions:

$$\phi_U^l = \phi_I^l + \tilde{\phi}_U^l, \tag{10}$$

The Fourier-Bessel series for $\tilde{\phi}_U^l$ is:

$$\tilde{\phi}_U^l = \sum_{n=1}^{\infty} e_n^l \left\{ E_n^l \frac{\cosh[\chi_n^l(z+d)]}{\cosh[\chi_n^l(h-d)]} + \frac{\sinh[\chi_n^l(z+h)]}{\cosh[\chi_n^l(h-d)]} \right\} \frac{J_l(\chi_n^l r)}{J_l'(\chi_n^l R_I)}, \tag{11}$$

where the constant E_n^l is:

$$E_n^l = \frac{\chi_n^l \cosh(\chi_n^l h) - f \sinh(\chi_n^l h)}{f \cosh(\chi_n^l d) - \chi_n^l \sinh(\chi_n^l d)}. \tag{12}$$

3 Results

A limiting case for comparison at $\tau = 1.0$ ($\Delta p = 0$), which represents the case without a dissipative disk, was employed to verify the accuracy of the analytical solution. For $\mu = 0$, the calculated internal wave motion in the moonpool agrees very well with Liu's [5], validating the model's accuracy (see Fig. 2).

The model effectively dampened internal oscillations by adding a dissipative disk with $\tau = 0.2$, proving the effectiveness of the suggested porous boundary condition.

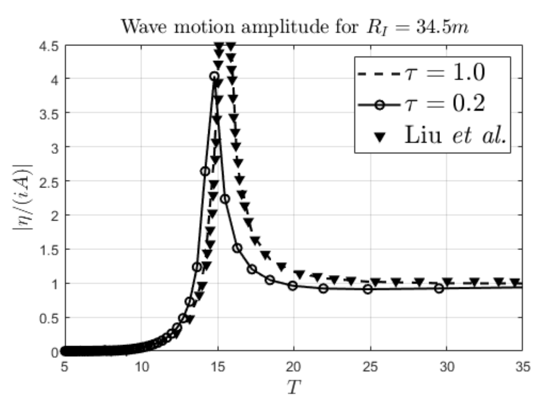

Figure 2: Wave motion amplitude in the moonpool for $R_I = 34.5\,\text{m}$.

To investigate the influence of moonpool geometry, simulations were performed for two radius ratios: $R_E/R_I = 2.0$ ($R_E = 69\,\text{m}$) and $R_E/R_I = 4.0$ ($R_E = 138\,\text{m}$). As shown in Figs. 3(a) and 3(b), increasing the exterior radius leads to a reduction in the peak amplitude.

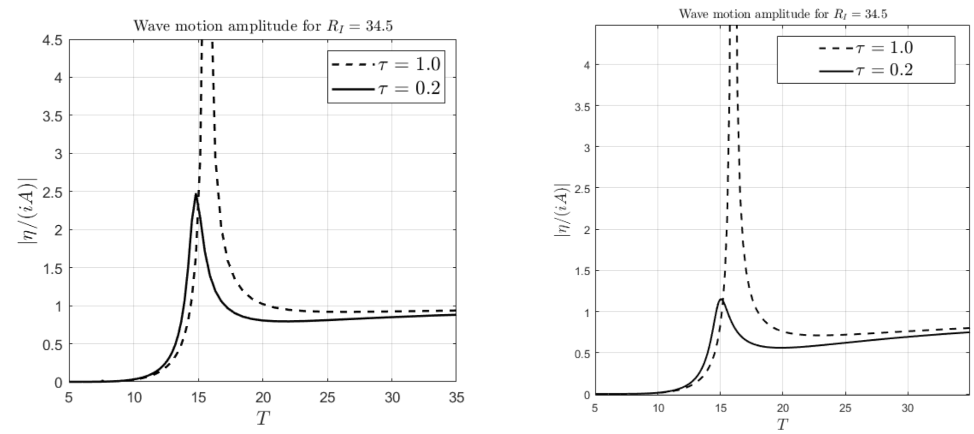

(a) $R_E/R_I = 2.0$ (b) $R_E/R_I = 4.0$

Figure 3: Motion of water column in the moonpool for different R_E/R_I ratios.

4 Conclusions

In this work, the effectiveness of the quadratic pressure drop condition was demonstrated by the effective damping of internal oscillations in the moonpool. The model provides a generalized, empirical-free method for future offshore engineering applications by introducing extra damping through a porous plate. More results regarding the free surface and wave loads will be discussed in the workshop.

REFERENCES

[1] Chen, Q., Cui, J., Feng, X., and Liu, Y. A new pressure drop model for porous plate in waves with consideration of boundary layer frictional effect. In *Proceedings of the 39th International Workshop on Water Waves and Floating Bodies* (St Andrews, Scotland, Apr. 2024). April 14–17.

[2] Miles, J., and Gilbert, F. 1968. *Scattering of gravity waves by a circular dock*. Journal of Fluid Mechanics 34(4), 783–793.

[3] Garrett, C. J. R. 1970. *Bottomless harbours*. Journal of Fluid Mechanics 43(3), 433–449.

[4] Mavrakos, S. A. 1985. *Wave loads on a stationary floating bottomless cylindrical body with finite wall thickness*. Applied Ocean Research 7(4), 213–224.

[5] Liu, H. X., Chen, H. L., Zhang, L., Zhang, W. C., and Liu, M. 2017. *Quadratic dissipation effect on the moonpool resonance*. China Ocean Engineering 31(6), 665–673.